

LU TP 98-30
December 1998

W Production in an Improved Parton-Shower Approach

Gabriela Miu¹ and Torbjörn Sjöstrand²

*Department of Theoretical Physics,
Lund University, Lund, Sweden*

Abstract

In the description of the production properties of gauge bosons (W^\pm, Z^0, γ^*) at colliders, the lowest-order graph normally is not sufficient. The contributions of higher orders can be introduced either by an explicit order-by-order matrix-element calculation, by a resummation procedure or by a parton-shower algorithm. Each approach has its advantages and disadvantages. We here introduce a method that allows the parton-shower algorithm to be augmented by higher-order information, thereby offering an economical route to a description of all event properties. It is tested by comparing with the p_\perp spectrum of W bosons at the Tevatron.

¹gabriela@hep.lu.se

²torbjorn@hep.lu.se

The W^\pm and Z^0 bosons have been extensively studied at colliders, in order to test the standard model [1]. In recent years they have also made their debut as backgrounds to other processes of interest: top studies, Higgs searches, and so on. Here it is often the association of the W/Z with one or several jets that is the source of concern. Such higher-order corrections to the basic processes also serve as tests of QCD. It is therefore of some interest to improve the accuracy with which gauge boson production can be described.

In this letter we will take the W^\pm production at hadron colliders as a test bed to develop some ideas in this direction. Specifically, we will discuss how to improve the lowest-order description $q\bar{q}' \rightarrow W^\pm$ by a merging of the first-order matrix elements $q\bar{q}' \rightarrow gW^\pm$ and $qg \rightarrow q'W^\pm$ with a leading-log parton shower. However, the formalism is valid for all colourless massive vector gauge bosons within and beyond the standard model: γ^* , Z^0 , Z'^0 , W'^\pm , and so on. It also applies e.g. in $e^+e^- \rightarrow \gamma Z^0$. One could in addition imagine extensions to quite different processes, such as Higgs production by $gg \rightarrow h^0$, but this would require further study.

The outline of the letter is the following. First we discuss various approaches to W production, and their respective limitations. Then we zoom in on the shower method and introduce a matrix-element-motivated method to improve it. Finally we compare with data, specifically the W transverse-momentum spectrum at the Tevatron, and draw some conclusions.

In essence, one may distinguish three alternative descriptions of W production:

1. *Order-by-order matrix elements.* By a systematic expansion in powers of α_s , a quite powerful machinery is obtained. For instance, there are calculations of the total Drell-Yan cross section to second order [2] and for the associated production of a W and up to four partons at the Born level [3]. A main problem is that there is no smooth transition between the different event classes, as one parton becomes soft or two partons collinear. The method is therefore better suited for exclusive questions than for an inclusive view of W event properties.
2. *Resummed matrix elements.* Here the effects of multiple parton emission are resummed, in impact-parameter or transverse-momentum space [4]. Inclusive quantities such as the $p_{\perp W}$ spectrum can be well described in such an approach, but it should be noted that a nonperturbative input is required. The standard formalism does not give the exclusive set of partons accompanying the W , however, and internally does not respect correct kinematics.
3. *Parton showers.* The parton-shower approach generates complete events, with correct kinematics. An arbitrary number of partons is obtained, with a smooth and physical transition between event classes ensured by the use of Sudakov form factors. On the other hand, the shower approach is formally only to leading-log accuracy (although many detailed choices are made to maximize agreement with next-to-leading-log results), and the description of the rate of exclusive parton configurations may be poor.

Finally, note that the perturbative partonic stage is not observable in experiment, but instead the hadronic jet one. Traditional hadronization descriptions, such as string fragmentation [5], are intended to be universal if applied at some low cut-off scale $Q_0 \sim 1$ GeV of the perturbative phase. This perfectly matches the shower approach, but causes problems in the use of matrix elements.

Given their complementary strengths, it is natural to attempt a marriage of the matrix-element and parton-shower methods, where the rate of well-separated jets is consistent with the former while the substructure of jets is described by the latter. The simpler

solution, *matching*, is to introduce a transition from one method to the other at some intermediate scale [6, 7, 8]. Such an approach is convenient for descriptions of exclusive jet topologies, but tend to suffer from discontinuities between event classes and around the transition scale. More ambitious is the *merging* strategy, where matrix-element information is integrated into the shower in such a way as to obtain a uniform and smooth description. This approach so far has only been implemented for the merging to $O(\alpha_s)$ of $e^+e^- \rightarrow q\bar{q}$ with $e^+e^- \rightarrow q\bar{q}g$ [9, 7]. We will here introduce a corresponding $O(\alpha_s)$ merging in hadronic W production. Further details may be found in [10].

Since we neglect the decay of the W, alternatively imagine it decaying leptonically, all QCD radiation occurs in the initial state. We will base our approach on the initial-state shower algorithm of [11], as implemented in PYTHIA [12]. The principle of *backwards evolution* implies that a shower may be reconstructed by starting at the large Q^2 scale of the hard process and then gradually considering emissions at lower and lower virtualities, i.e. earlier and earlier in the cascade chain (and in time).

The starting point is the standard DGLAP evolution equation [13],

$$\frac{df_b(x, t)}{dt} = \sum_a \int_x^1 \frac{dx'}{x'} \frac{\alpha_s(t)}{2\pi} f_a(x', t) P_{a \rightarrow bc}(z) , \quad (1)$$

with f_i the distribution function of parton species i , x the momentum fraction carried by the parton, $t = \ln(Q^2/\Lambda_{\text{QCD}}^2)$ the resolution scale, and $P_{a \rightarrow bc}(z)$ the AP splitting kernels for parton b obtaining a fraction $z = x/x'$ of the a momentum. Normally the evolution is in terms of increasing t , but in the backwards evolution t is instead decreasing. Then the DGLAP equation expresses the rate at which partons b of momentum fraction x are ‘unresolved’ into partons a of fraction x' , in a step dt backwards. The corresponding relative probability is $dP_b/dt = (1/f_b) (df_b/dt)$. The probability that b remains resolved from some initial scale t_{\max} down to $t < t_{\max}$ is thereby obtained by a Sudakov form factor

$$\begin{aligned} S_b(x, t; t_{\max}) &= \exp \left(- \int_t^{t_{\max}} \frac{1}{f_b(x, t')} \frac{df_b(x, t')}{dt'} dt' \right) \\ &= \exp \left(- \int_t^{t_{\max}} dt' \sum_a \int_x^1 \frac{dx'}{x'} \frac{\alpha_s(t')}{2\pi} \frac{f_a(x', t')}{f_b(x, t')} P_{a \rightarrow bc}(z) \right) \\ &= \exp \left(- \int_t^{t_{\max}} dt' \frac{\alpha_s(t')}{2\pi} \sum_a \int_x^1 dz \frac{x' f_a(x', t')}{x f_b(x, t')} P_{a \rightarrow bc}(z) \right) . \end{aligned} \quad (2)$$

From this expression it is a matter of standard Monte Carlo techniques to generate the complete branching $a \rightarrow bc$ [11]; e.g., the t distribution of the branching is $-dS_b(x, t; t_{\max})/dt$. Given parton a , one may in turn reconstruct which parton branched into it, and so on, down to the starting scale Q_0 . In each branching, the t scale gives the t_{\max} value of the branching to be considered next, i.e. the Q^2 values are assumed strictly ordered.

The definition of the Q^2 and z variables is not unambiguous. Referring to the notation of Fig. 1, and to the branching $3 \rightarrow 1 + 4$, the Q^2 scale in our algorithm [11] is associated with the spacelike virtuality of the produced parton 1, $Q^2 = -p_1^2$, while z is given by the reduction of squared invariant mass of the contained subsystem, $z = (p_1 + p_2)^2/(p_3 + p_2)^2$. In the limit of collinear kinematics, $Q^2 = 0$, one recovers the momentum fraction $z = p_1/p_3$. The z definition couples the two sides of the events, so that the order in which the branchings $3 \rightarrow 1 + 4$ and $5 \rightarrow 2 + 6$ are considered makes some difference for the final

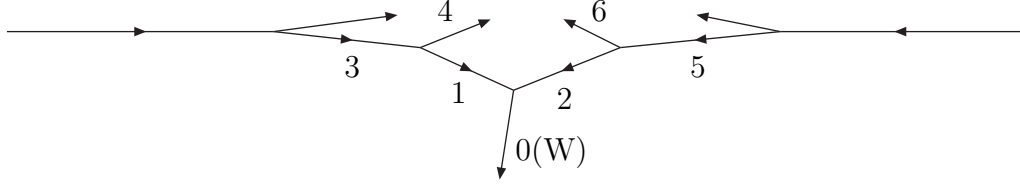


Figure 1: Schematic picture of an initial-state parton shower, extending from both sides of the event in to the W .

configuration. The rule adopted is therefore to reconstruct branching kinematics strictly in order of decreasing Q^2 , i.e. interleaving emissions on the two sides of the event.

Now let us compare the step from $q\bar{q}' \rightarrow W$ to $q\bar{q}' \rightarrow gW$ between the matrix-element and parton-shower languages. Since only one branching is to be considered, the comparison has to be with a truncated shower, e.g. where only the branching $3 \rightarrow 1 + 4$ occurs in Fig. 1. The $2 \rightarrow 2$ process thus is $q(3) + \bar{q}'(2) \rightarrow g(4) + W(0)$, for which

$$\begin{aligned}\hat{s} &= (p_3 + p_2)^2 = \frac{(p_1 + p_2)^2}{z} = \frac{m_W^2}{z}, \\ \hat{t} &= (p_3 - p_4)^2 = p_1^2 = -Q^2, \\ \hat{u} &= m_W^2 - \hat{s} - \hat{t} = Q^2 - \frac{1-z}{z} m_W^2.\end{aligned}\quad (3)$$

The matrix element for $q\bar{q}' \rightarrow gW$ can be written as [14]

$$\frac{d\hat{\sigma}}{d\hat{t}} \Big|_{\text{ME}} = \frac{\sigma_0}{\hat{s}} \frac{\alpha_s}{2\pi} \frac{4}{3} \frac{\hat{t}^2 + \hat{u}^2 + 2m_W^2\hat{s}}{\hat{t}\hat{u}}. \quad (4)$$

Here σ_0 is the cross section for $q\bar{q}' \rightarrow W$, $\sigma_0 = (\pi^2\alpha_{\text{em}}/3 \sin^2\theta_W m_W^2) |V_{q\bar{q}'}|^2 \delta(1-m_W^2/x_1 x_2 s)$ in the narrow-width limit, with $\delta(1-m_W^2/x_1 x_2 s) \mapsto \int dz \delta(1-m_W^2/z x_3 x_2 s)$ in the $2 \rightarrow 2$ process kinematics. (The details of the σ_0 factor are not relevant for the point we want to make, so the presentation is intentionally sketchy.) Now rewrite eq. (4) in terms of z and Q^2 , using eq. (3):

$$\begin{aligned}\frac{d\hat{\sigma}}{dQ^2} \Big|_{\text{ME}} &= \frac{\sigma_0 z}{m_W^2} \frac{\alpha_s}{2\pi} \frac{4}{3} \frac{(1+z^2)m_W^4 - 2z(1-z)Q^2m_W^2 + 2z^2Q^4}{zQ^2((1-z)m_W^2 - zQ^2)} \\ &\xrightarrow{Q^2 \rightarrow 0} \sigma_0 \frac{\alpha_s}{2\pi} \frac{4}{3} \frac{1+z^2}{1-z} \frac{1}{Q^2} = \frac{d\hat{\sigma}}{dQ^2} \Big|_{\text{PS1}}.\end{aligned}\quad (5)$$

We here easily recognize the splitting kernel for $q \rightarrow qg$, i.e. the matrix element reduces to the the normal shower expression in the collinear limit, as it should be. Some extra but trivial work is necessary to include the convolution with parton distributions, which involves $f_1(x_1, Q^2)$ in lowest order and $f_3(x_3, Q^2)$ for the $O(\alpha_s)$ processes.

In order to study how the shower populates the phase space, it is straightforward to translate back the above expression,

$$\frac{d\hat{\sigma}}{d\hat{t}} \Big|_{\text{PS1}} = \frac{\sigma_0}{\hat{s}} \frac{\alpha_s}{2\pi} \frac{4}{3} \frac{\hat{s}^2 + m_W^4}{\hat{t}(\hat{t} + \hat{u})}. \quad (6)$$

To this we should add the other possible shower history, where the gluon is emitted by a branching $5 \rightarrow 2 + 6$ instead; after all, the matrix-element expression contains both

amplitudes. The collinear singularity $Q^2 \rightarrow 0$ here corresponds to emission along direction 2 rather than direction 1. In that case the rôles of \hat{t} and \hat{u} are interchanged, and the cross section $d\hat{\sigma}/d\hat{t}|_{PS2}$ is easily obtained. The total shower rate is given by the sum,

$$\frac{d\hat{\sigma}}{d\hat{t}} \Big|_{PS} = \frac{d\hat{\sigma}}{d\hat{t}} \Big|_{PS1} + \frac{d\hat{\sigma}}{d\hat{t}} \Big|_{PS2} = \frac{\sigma_0}{\hat{s}} \frac{\alpha_s}{2\pi} \frac{4}{3} \frac{\hat{s}^2 + m_W^4}{\hat{t}\hat{u}} . \quad (7)$$

Thus the singularity structure of the parton-shower and matrix-element rates agree, giving a ratio

$$R_{q\bar{q}' \rightarrow gW}(\hat{s}, \hat{t}) = \frac{(d\hat{\sigma}/d\hat{t})_{ME}}{(d\hat{\sigma}/d\hat{t})_{PS}} = \frac{\hat{t}^2 + \hat{u}^2 + 2m_W^2\hat{s}}{\hat{s}^2 + m_W^4} = 1 - \frac{2\hat{t}\hat{u}}{\hat{s}^2 + m_W^4} \quad (8)$$

constrained to the range

$$\frac{1}{2} < R_{q\bar{q}' \rightarrow gW}(\hat{s}, \hat{t}) \leq 1 . \quad (9)$$

The same exercise may be carried out for $qg \rightarrow q'W$:

$$\begin{aligned} \frac{d\hat{\sigma}}{d\hat{t}} \Big|_{ME} &= \frac{\sigma_0}{\hat{s}} \frac{\alpha_s}{2\pi} \frac{1}{2} \frac{\hat{s}^2 + \hat{u}^2 + 2m_W^2\hat{t}}{-\hat{s}\hat{u}} \\ &= \frac{\sigma_0 z}{m_W^2} \frac{\alpha_s}{2\pi} \frac{1}{2} \frac{(z^2 + (1-z)^2)m_W^4 + 2z^2Q^2m_W^2 + z^2Q^4}{zQ^2m_W^2} \\ &\xrightarrow{Q^2 \rightarrow 0} \sigma_0 \frac{\alpha_s}{2\pi} \frac{1}{2} (z^2 + (1-z)^2) \frac{1}{Q^2} = \frac{d\hat{\sigma}}{dQ^2} \Big|_{PS} , \end{aligned} \quad (10)$$

$$\frac{d\hat{\sigma}}{d\hat{t}} \Big|_{PS} = \frac{\sigma_0}{\hat{s}} \frac{\alpha_s}{2\pi} \frac{1}{2} \frac{\hat{s}^2 + 2m_W^2(\hat{t} + \hat{u})}{-\hat{s}\hat{u}} , \quad (11)$$

$$R_{qg \rightarrow q'W}(\hat{s}, \hat{t}) = \frac{(d\hat{\sigma}/d\hat{t})_{ME}}{(d\hat{\sigma}/d\hat{t})_{PS}} = \frac{\hat{s}^2 + \hat{u}^2 + 2m_W^2\hat{t}}{\hat{s}^2 + 2m_W^2(\hat{t} + \hat{u})} = 1 + \frac{\hat{u}(\hat{u} - 2m_W^2)}{(\hat{s} - m_W^2)^2 + m_W^4} , \quad (12)$$

$$1 \leq R_{qg \rightarrow q'W}(\hat{s}, \hat{t}) \leq \frac{\sqrt{5} - 1}{2(\sqrt{5} - 2)} < 3 . \quad (13)$$

Note that, unlike the $q\bar{q}' \rightarrow gW$ process, there is no addition of two shower histories when comparing with matrix elements, since here also the latter contains two separate terms corresponding to qg and gq initial states, respectively.

The $q\bar{q}' \rightarrow gW$ process receives contributions from two Feynman graphs, t -channel and u -channel, and the shower thus exactly matches this set, although obviously it does not include interference between the two. The $qg \rightarrow q'W$ process is different, since only its u -channel graph is covered by the parton-shower formalism, while the s -channel one has no correspondence. Since this latter graph is free from collinear singularities, the shower is not misbehaving in any regions of phase space because of this omission, but it is interesting to speculate that the larger value for $R_{qg \rightarrow q'W}(\hat{s}, \hat{t})$ than for $R_{q\bar{q}' \rightarrow gW}(\hat{s}, \hat{t})$ partly may have its origin here (remember that a larger $R(\hat{s}, \hat{t})$ means a smaller shower emission rate).

Based on the above exercise, the standard parton-shower approach may be improved in two steps. The first is to note that, since the shower so closely agrees with the correct matrix-element expression — much better than one might have had reason to expect — it is safe to apply the shower to all of phase space, i.e. to have $Q_{\max}^2 \approx s$ rather than the more traditional shower-generator limit $Q_{\max}^2 \approx m_W^2$ [12, 8]. The older choice was inspired in part by the fear of a completely erroneous behaviour for $Q^2 \gg m_W^2$, in part by

the typical factorization scale used for parton distributions in W cross-section formulae. Such a scale choice can be motivated by doublecounting arguments. Most easily this is seen in pure QCD processes, where a $2 \rightarrow 3$ process such as $gg \rightarrow q\bar{q}g$ could be obtained starting from several different $2 \rightarrow 2$ processes, and classification by the hardest (most virtual) subgraph is necessary to resolve ambiguities. Correspondingly, a W production graph could be reclassified once some parton has $Q^2 > m_W^2$. That is, in general, one would have to consider QCD processes where the emission of a W is allowed as a ‘parton shower’ correction. (The s -channel graph in $qg \rightarrow q'W$ is an example of this kind.) Doublecounting is not an issue, however, once we decide to represent the full W cross section by $q\bar{q} \rightarrow W$. (Remember that the shower does not change total cross sections.)

The second step is to use standard Monte Carlo techniques to correct branchings in the shower by the relevant ratio $R(\hat{s}, \hat{t})$, to bring the shower parton-emission rate in better agreement with the matrix-element one. This correction is applied to the branching closest to the hard scattering, i.e. with largest virtuality, on both sides of the event, i.e. for $3 \rightarrow 1 + 4$ and $5 \rightarrow 2 + 6$ in Fig. 1. By analogy with results for time-like showers [7], one could attempt to formulate more precise rules for when to apply corrections, but this one should come close enough and is technically the simplest solution. (For instance, while our cascade is ordered in Q^2 rather than in p_\perp^2 , the emission with largest p_\perp^2 normally coincides with the largest Q^2 one, so either criterion for when to apply a correction would give very similar results.) For a $q \rightarrow qg$ shower branching, where the correction factor $R(\hat{s}, \hat{t}) = R_{q\bar{q}' \rightarrow gW}(\hat{s}, \hat{t}) \leq 1$, a candidate branching selected according to the Sudakov factor in eq. (2) is then accepted with a probability $R(\hat{s}, \hat{t})$. In case of failure, the evolution downwards in Q^2 is continued from the scale that failed (the ‘veto algorithm’, ensuring the correct form of the Sudakov). For a $g \rightarrow q\bar{q}$ branching, the fact that $R(\hat{s}, \hat{t}) = R_{qg \rightarrow q'W}(\hat{s}, \hat{t}) \geq 1$ means that the procedure above cannot be used directly. Instead the normal $g \rightarrow q\bar{q}$ branching rate is enhanced by an ad hoc factor of 3, and the acceptance rate instead given by $R(\hat{s}, \hat{t})/3 < 1$.

Even with this injection of matrix-element information into the parton shower, it is important to recognize that the shower still is different. The hardest emission is given by the matrix-element expression *times* the related Sudakov form factor, thus ensuring a smooth p_\perp spectrum that vanishes in the limit $p_\perp \rightarrow 0$. By the continued shower history (without any matrix-element corrections), further emissions pick up where the Sudakov factor suppresses the hardest one, giving a total p_\perp spectrum of emitted partons that is peaked at the lower p_\perp cut. This total spectrum is similar to the matrix-element one, but deviates from it in that the shower includes kinematical and dynamical effects of gradually having partons at larger and larger x values and possibly of different species at each softer emission. In some respects, it thus provides a more sophisticated approach to resummation for the properties of the recoiling W . It also gives exclusive final states, including the possibility for the emitted partons (such as 4 and 6 in Fig. 1) to branch in their turn.

The parton shower redistributes the W ’s in phase space but does not change the total W cross section. It is thus feasible to use a higher-order calculation of this cross section as starting point, although we did not do it here. If higher orders enhance the total cross section by a factor K (with K a function e.g. of rapidity) relative to the lowest-order $q\bar{q}' \rightarrow W$ one, the implication of eqs. (4) and (10) is that the one-jet rate is enhanced by the same factor. If instead another factor K' is wanted here, the respective $R(\hat{s}, \hat{t})$ weight could then be modified by a factor K'/K . Note, however, that it is more difficult to introduce such a K'/K factor consistently, since it presupposes a common definition

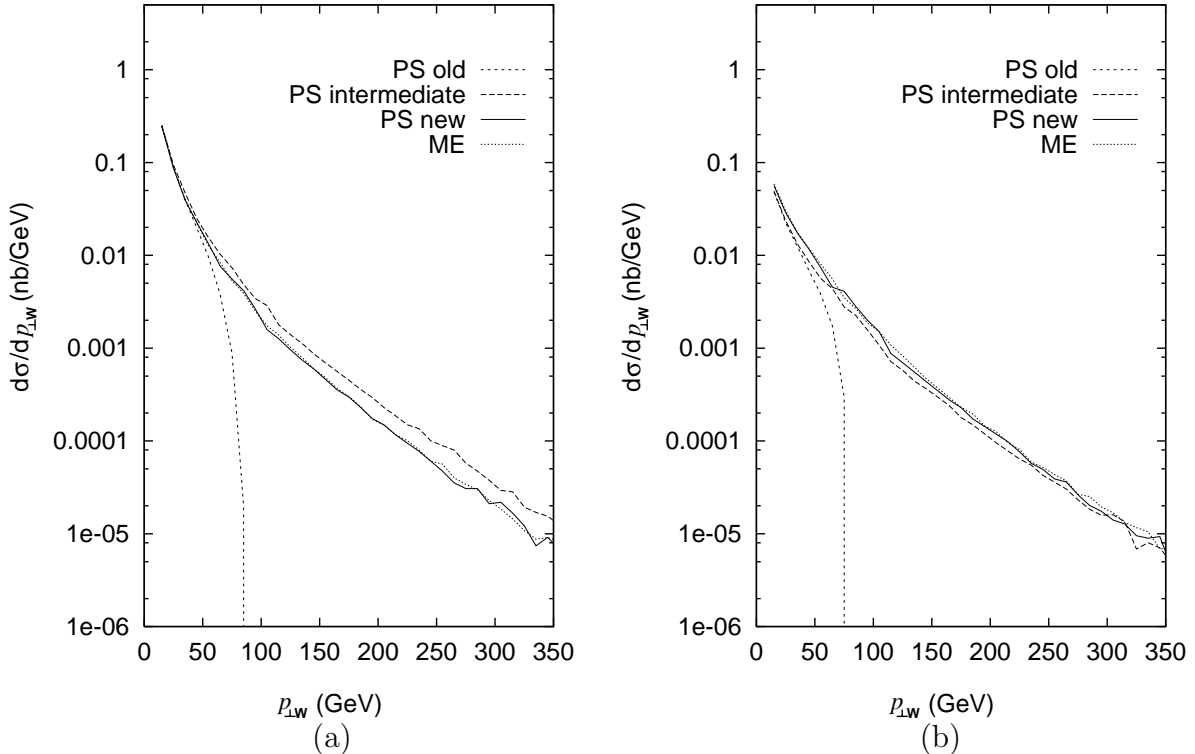


Figure 2: The $p_{\perp W}$ distribution in $p\bar{p}$ collisions at 1.8 TeV. Parton distributions and α_s are frozen and only one emission at a time is allowed in the shower. Events are classified either as (a) $q\bar{q}' \rightarrow gW$ or (b) $qg \rightarrow q'W$.

between showers and matrix elements of what constitutes a jet.

As a first check, we want to confirm that the shower algorithm works as intended, reproducing the matrix-element expressions where it should. Thus the shower is artificially modified so as only to generate one branching at a time. In order to eliminate the influence of the Sudakov and the change of kinematics by previously considered emissions, the shower is restarted from each Q^2 actually selected above the cut, but returning to the original kinematics for $q\bar{q}' \rightarrow W$. Furthermore parton distributions and α_s are frozen, so as to avoid any scale-choice mismatches. The resulting W transverse momentum spectrum is shown in Fig. 2, classified by the two possible branchings. In the old scheme, with $Q_{\max}^2 = m_W^2$, the drop of the $p_{\perp W}$ spectrum at $p_{\perp W} \approx m_W$ is easily visible. Already the modification to $Q_{\max}^2 = s$ (the ‘intermediate’ curves) brings a marked improvement, and the further introduction of the $R(\hat{s}, \hat{t})$ weighting (‘new’) results in good agreement between the shower and the matrix elements.

The $R(\hat{s}, \hat{t})$ factors are further studied in Fig. 3. It is seen that $R(\hat{s}, \hat{t})$ is close to unity for most of the branchings (note the logarithmic scale). Also that $R(\hat{s}, \hat{t}) \rightarrow 1$ as $p_{\perp} \rightarrow 0$, in accordance with the demonstrated agreement of the parton shower and matrix elements in the collinear limit. At large p_{\perp} values, the $R(\hat{s}, \hat{t})$ factors enhance the importance of the $qg \rightarrow q'W$ process relative to the $q\bar{q}' \rightarrow gW$ one by about a factor of 2. When the two processes are not separated, the partial cancellation of having one $R(\hat{s}, \hat{t})$ a bit above unity and the other a bit below leads to a rather modest net correction to p_{\perp} spectra.

We now present results for the new parton shower, in all its complexity, i.e. with normal complete showers augmented by the two-step correction process described above. In Fig. 4 the shower $p_{\perp W}$ distribution is compared with experimental data from the

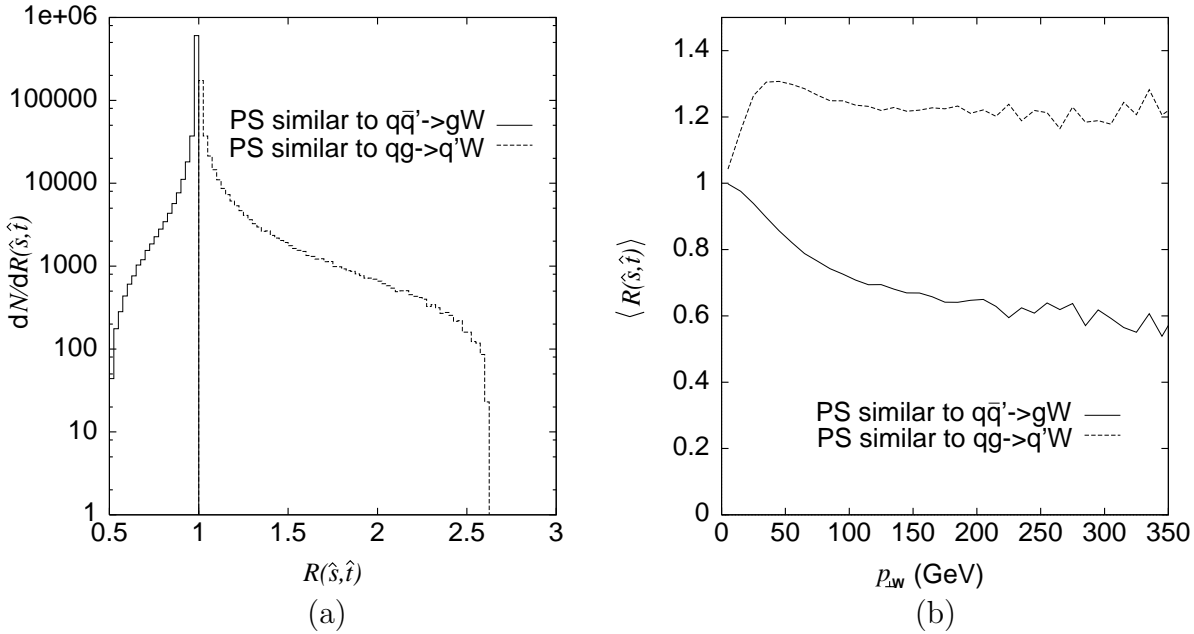


Figure 3: $R(\hat{s}, \hat{t})$ distributions in $p\bar{p}$ collisions at 1.8 TeV. (a) The inclusive distribution. (b) The average value as a function of $p_{\perp W}$. Events are classified either as $q\bar{q}' \rightarrow gW$ or $qg \rightarrow q'W$.

D0 collaboration [15]. The agreement is good for large $p_{\perp W}$, but the shape at small $p_{\perp W}$ is rather different, with less activity in the shower than in data. These results are for the default Gaussian primordial k_{\perp} spectrum of width 0.44 GeV, as would be the order expected from a purely nonperturbative source related to confinement inside the incoming hadrons. By now several indications have accumulated that a larger width is needed, however [16], although the origin of such an excess is not at all understood. One hypothesis is that some radiation is overlooked by an imperfect modelling of the perturbative QCD radiation around or below the Q_0 cut-off scale. Whatever the reason, we may quantify the disagreement by artificially increasing the primordial k_{\perp} width. Fig. 4 shows that an excellent agreement can be obtained, at all $p_{\perp W}$ values, with a 4 GeV width. The $p_{\perp W}$ distribution is essentially unchanged at large values, i.e. only the region $p_{\perp W} \lesssim 20$ GeV is affected. In order to put the 4 GeV number in perspective, it should be noted that this is introduced as a ‘true’ primordial k_{\perp} , i.e. carried by the parton on each incoming hadron side that initiates the initial-state shower at the Q_0 scale. If such a parton has an original momentum fraction x_0 and the parton at the end of the cascade (that actually produces the W) has fraction x , the W only receives a primordial k_{\perp} kick scaled down by a factor x/x_0 . In the current case, and also including the fact that two sides contribute, this translates into a rms width of 2.1 GeV for the primordial k_{\perp} kick given to the W. This number actually is not so dissimilar from values typically used in resummation descriptions [4].

In summary, we see that it is possible to obtain a good description of the complete $p_{\perp W}$ spectrum by fairly straightforward improvements of a normal parton-shower approach. Corresponding improvements can also be expected for the production of jets in association with the W. Especially, the good matching offered to hadronization descriptions in this approach allows a complete simulation of the final state, including the addition of a (possibly process-dependent) underlying event. This way it should be possible to address e.g. the ratio of events with/without a jet accompanying the W, where CDF and D0 have

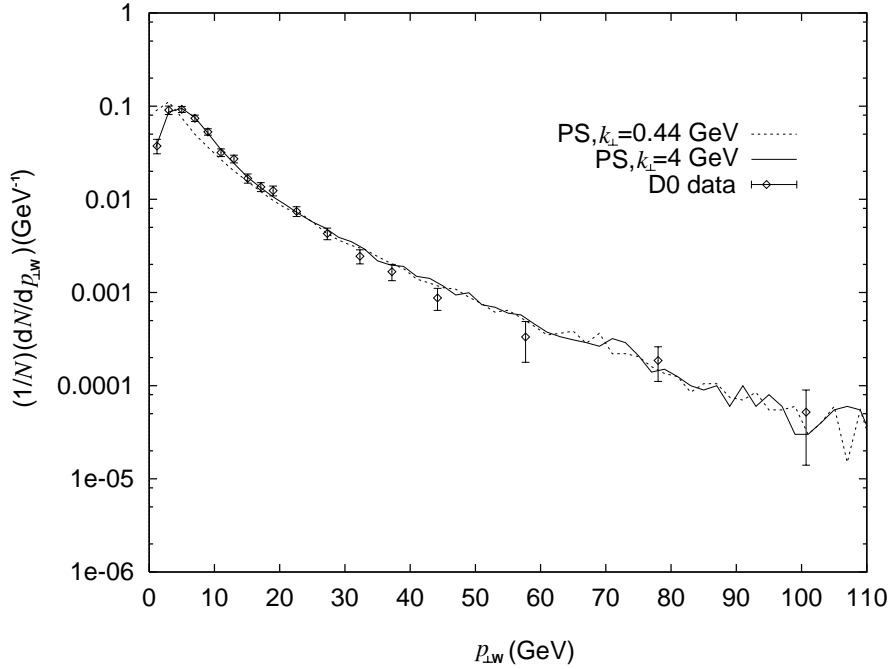


Figure 4: Transverse momentum spectrum of the W; full parton-shower results compared with data from the D0 Collaboration [15]. (The error bars include both statistical and systematic uncertainties.)

obtained partly conflicting results, however using different jet definitions [17].

We end by reiterating that the formalism presented here is universal, in the sense that the formulae in this paper are not unique for the W, but shared by all vector gauge bosons, after an appropriate replacement of m_W and the constants in the σ_0 prefactor. Specifically, the reweighting factors $R(\hat{s}, \hat{t})$ need only be modified to reflect the mass of the current resonance. The method therefore should offer an accurate and economical route to the prediction of kinematical distributions for a host of new particles, to be searched for at the Tevatron and the LHC. It is also likely that similar approaches can be developed for other classes of processes.

References

- [1] Particle Data Group, C. Caso et al., Eur. Phys. J. **C3** (1998) 1.
- [2] R. Hamberg, W.L. van Neerven, T. Matsuura, Nucl. Phys. **B359** (1991) 343; W.L. van Neerven and E.B. Zijlstra, Nucl. Phys. **B382** (1992) 11.
- [3] F.A. Berends, H. Kuijf, B. Tausk and W.T. Giele, Nucl. Phys. **B357** (1991) 32.
- [4] Yu.L. Dokshitzer, D.I. Dyakonov and S.I. Troyan, Phys. Rep. **58** (1980) 269; F. Halzen, A.D. Martin, D.M. Scott and M.P. Tuite, Z. Phys. **C14** (1982) 351; G. Altarelli, R.K. Ellis, M. Greco and G. Martinelli, Nucl. Phys. **B246** (1984) 12; J.C. Collins, D.E. Soper and G. Sterman, Nucl. Phys. **B250** (1985) 199; C.T.H. Davies, B.R. Webber and W.J. Stirling, Nucl. Phys. **B256** (1985) 413; P.B. Arnold and R. Kauffman, Nucl. Phys. **B349** (1991) 381;

G.A. Ladinsky and C.-P. Yuan, Phys. Rev. **D50** (1994) 4239;
 R.K. Ellis and S. Veseli, Nucl. Phys. **B511** (1998) 649.

[5] B. Andersson, G. Gustafson, G. Ingelman and T. Sjöstrand, Phys. Rep. **97** (1983) 31.

[6] H. Baer and M.H. Reno, Phys. Rev. **D44** (1991) 3375;
 J. André and T. Sjöstrand, Phys. Rev. **D57** (1998) 5767;
 F.E. Paige, S.D. Protopopescu, H. Baer and X. Tata, hep-ph/9810440.

[7] M.H. Seymour, Computer Phys. Commun. **90** (1991) 95.

[8] G. Marchesini, B.R. Webber, G. Abbiendi, I.G. Knowles, M.H. Seymour and L. Stanco, Computer Phys. Commun. **67** (1992) 465.

[9] M. Bengtsson and T. Sjöstrand, Phys. Lett. **B185** (1987) 435;
 G. Gustafson and U. Pettersson, Nucl. Phys. **B306** (1988) 746.

[10] G. Miu, LU TP 98-9, hep-ph/9804317.

[11] T. Sjöstrand, Phys. Lett. **157B** (1985) 321;
 M. Bengtsson, T. Sjöstrand and M. van Zijl, Z. Phys. **C32** (1986) 67.

[12] T. Sjöstrand, Computer Phys. Commun. **82** (1994) 74.

[13] V.N. Gribov and L.N. Lipatov, Sov. J. Nucl. Phys. **15** (1972) 438;
 G. Altarelli and G. Parisi, Nucl. Phys. **B126** (1977) 298;
 Yu.L. Dokshitzer, Sov. Phys. JETP **46** (1977) 641.

[14] H. Fritzsch and P. Minkowski, Phys. Lett. **73B** (1978) 80;
 G. Altarelli, G. Parisi and R. Petronzio, Phys. Lett. **76B** (1978) 351;
 K. Kajantie and R. Raitio, Nucl. Phys. **B139** (1978) 72;
 F. Halzen and D.M. Scott, Phys. Rev. **D18** (1978) 3378.

[15] CDF Collaboration, F. Abe et al., Phys. Rev. Lett. **66** (1991) 2951;
 D0 Collaboration, B. Abbott et al., Phys. Rev. Lett. **80** (1998) 5498.

[16] S. Frixione, M.L. Mangano, P. Nason and G. Ridolfi, Nucl. Phys. **B431** (1994) 453;
 L. Apanasevich et al., hep-ph/9808467.

[17] D0 Collaboration, B. Abbott et al., FERMILAB-Conf-97/369-E;
 CDF Collaboration, F. Abe et al., Phys. Rev. Lett. **81** (1998) 1367.